Proceedings of the Institute of Acoustics

MODELLING OF OMNIDIRECTIONAL RESPONSE OF AN HYDROPHONE IN SHALLOW WATER REFLECTING SEABED

H Dupuis and A Weill

Centre de Recherche en Physique de l'Environnement, Issy les Moulineaux, France

1. INTRODUCTION

During an hydrophone experiment set up at Trebeurden (France) in october 1990 to interpret physical parameters of the air-sea interface in shallow water, unusual noise mean levels relatively to wind intensity were observed even at high frequencies. Intense discrete sources near the coast farther than the listening area have been suspected to have enough efficiency to be registered at the hydrophone location implying possible effects of seabed reflection on sound propagation.
This theoretical study concerns the response of an hydrophone as function of depth and frequency taking into account seabed reflection. It aims to describe and delimit the surface area acoustically observed, in terms of weighting function and listening radius, as defined by Farmer and Vagle [1], to make easier interpretation of physical parameters of the sea surface. Following Chapman [2] who used the method of image to obtain noise intensity received per unit angle in presence of a reflecting bottom, we have added the effect of water absorption (refraction is not considered). The seabed reflectivity function is estimated for two typical configurations where the ocean is described by a three layers structure: water/sediment/subbottom as defined in [3]. We will first describe the method and then the numerical simulations of omnidirectional noise carried out for different frequencies in the range from 100 Hz to 20 kHz and at different depth configurations (ocean and hydrophone depth). They provide an estimation of parameters describing the spatial influence of sources at the sea surface that we will comment as function of depth, frequency and bottom characteristics. At last, we discuss modelled noise spectra.

2. METHOD OF ANALYSIS

In this theoretical approach one considers acoustic sources as uniformly distributed at the surface and we try to estimate the surface weighting function above an hydrophone. Following Farmer and Vagle [1], the weighting function is the relative strength of a contribution to the sound spectrum level from the surface source as a function of range. To determine the relative importance of sources at the sea surface as a function of depth, bottom characteristics and frequency, we have first computed the intensity at the receiver per unit solid angle for the different parameters, see figure 2.1(a). The final sound intensity, to be compared to experimental results, is omnidirectional but takes into account the sources and bottom reflectivity directivity functions. It corresponds to the integral of intensity received per solid angle over 4π steradians, provided that the waves arriving from different directions are uncorrelated. When the bottom reflection is not considered, this method is equivalent to Farmer & Vagle's method [1] without refraction, hence it should be more realistic for shallow water, where bottom influence should be more important than refraction. As a remark, we need only to consider the directivity dependence in a vertical plane because the noise will be independent of direction in the horizontal plane.

2.1 Estimation of the omnidirectional intensity

A simple method is described by Chapman [2] to determine noise intensity per unit solid angle and

HYDROPHONE RESPONSE MODELLING

can be analyzed in several stages:

-First we consider a no reflecting seabottom. We assume wind and waves conditions leading to σ sources per unit surface area, each radiating acoustic power P at a given frequency f, and the source directivity function being the dipole function: $S(\theta)=\cos^2(\theta)$.

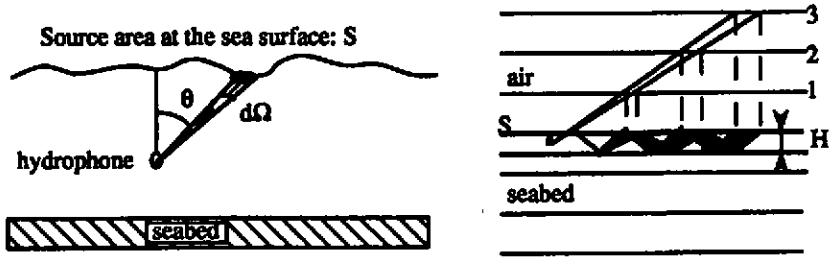

Figure 2.1:Configuration of intensity received per unit solid angle, (a) without bottom reflection, (b) using the method of image to account for noise arriving via multiple bounces.

As shown by Cox [4], the intensity received per unit solid angle, for an unreflecting seabed is of course zero for inclinaison angles θ (θ is referred to the surface normal) greater than 90°, see figure 2.1(a). For angles less than 90°, the intensity coming from surface sources is:

$$I_0(\theta) = \frac{\sigma P S(\theta)}{2\pi\cos\theta} \qquad (1)$$

This result takes into account the spherical spreads of acoustic intensity but neglects absorption in the water that we analyze later.

-Then we now consider the effect of a reflecting bottom, by using the method of images as described by Chapman in [2]: Noise intensity $I_n(\theta)$, received from direction θ after n reflections along a multilinear path is equivalent to intensity along a linear path, arriving in the same direction from a source located on the n^{th} image plane. (see figure 2.1(b))

Then $I_n(\theta)=I_0(\theta)R^n(\theta)$, where $R(\theta)$ is the bottom reflectivity function and the total intensity received per unit solid angle is due to all image sources coming from this direction:

$$I(\theta) = \sum_{n=0}^{\infty} I_n(\theta) \quad \text{for } \theta < 90° \quad \text{and} \quad I(\theta) = \sum_{n=1}^{\infty} I_n(\theta) \quad \text{for } \theta > 90° \qquad (2,3)$$

To be more realistic, we have also considered water absorption with α the absorption coefficient in db/m as a function of frequency. We have observed that the intensity from the n^{th} image source is $I_n(\theta)=I_0(\theta)R^n(\theta)$. This intensity will be reduced proportionally to the length of the paths, hence we have to introduce H the depth of the ocean and h the depth of the hydrophone. For waves in coming above the horizontal plane (for $\theta<90°$), the n^{th} image plane is located at 2nH above the surface, therefore for a ray propagating in direction θ, the intensity is divided by: $\exp(\alpha(2nH+h)/\cos\theta)$.

and:
$$I(\theta) = I_0(\theta) \sum_{n=0}^{\infty} \exp\left(-\alpha\left(\frac{2nH+h}{\cos\theta}\right)\right) R^n(\theta) = I_0(\theta) \exp\left(\frac{-\alpha h}{\cos\theta}\right) \frac{1}{1 - R(\theta)\exp\left(\frac{-2\alpha H}{\cos\theta}\right)} \qquad (4)$$

For waves coming below the horizontal plane (for $\theta>90°$), the n^{th} image plane is located $2(n-1)H+H$ below the bottom and:

HYDROPHONE RESPONSE MODELLING

$$I(\theta) = I_0(\theta) \sum_{n=1}^{\infty} \exp\left(-\alpha\left(\frac{2nH-h}{\cos\theta}\right)\right) R^n(\theta) = I_0(\theta) \exp\left(\frac{\alpha h}{\cos\theta}\right) \frac{R(\theta)\exp\left(\frac{-\alpha 2H}{\cos\theta}\right)}{1 - R(\theta)\exp\left(\frac{-2\alpha H}{\cos\theta}\right)} \quad (5)$$

-Finally we discuss the bottom reflectivity function with a method based on a geometrical acoustic approximation. We consider the ocean and its bottom as a three homogeneous layers structure: water/sediment/subbottom. Two typical seabed configurations have been studied, one with high contrasts of velocities and densities, e.g. a sandy layer above a basaltic subbottom, the other with lower contrasts, e.g. a thick layer over a subbottom whose properties are not very different [3], in such a way to match realistic conditions which can occur in our experiments.

The sediment is a fluid of thickness d, density ρ_2, where compressional waves are propagated with velocity c_2 and attenuation coefficient α_2 (dB/m.kHz). The subbottom is a solid of density ρ_3 and infinite thickness supporting compressional waves (velocity c_p, attenuation coefficient α_p) and shear waves (velocity c_s , attenuation coefficient α_s).The corresponding values are listed in table 2.1.

FIRST CONFIGURATION : HIGH CONTRASTS					
	ρ (kg/m^3)	c_p (m/s)	c_s (m/s)	α_p (dB/m/kHz)	α_s (dB/m/kHz)
WATER	1000	1500	0	0	0
SEDIMENT	1920	1700	0	0.1	0
SOLID	2200	4000	2000	0.01	0.3
SECOND CONFIGURATION : LOW CONTRASTS					
WATER	1000	1500	0	0	0
SEDIMENT	1400	1550	0	0.1	0
SOLID	1800	1650	400	0.3	2

Table 2.1: Physical parameters describing seabed characteristics from [3]

If we consider a monochromatic plane wave generated in the water and propagating downward at inclination angle θ, multiple reflections and transmissions occur as shown on figure 2.2.

The total reflection coefficient $R(\omega,\theta)$ is, see for example Brekhovskikh [5]:

$$R(\omega,\theta) = \frac{R_{12} + R_{23}e^{2jk_{2z}d}}{1 + R_{12}R_{23}e^{2jk_{2z}d}} \quad (6)$$

Where: $R_{12} = \frac{\rho_2 k_{1z} - \rho_1 k_{2z}}{\rho_2 k_{1z} + \rho_1 k_{2z}}$, $R_{23} = \frac{\rho_3 k_{2z} L - \rho_2 k_{3z} k_s^4}{\rho_3 k_{2z} L + \rho_2 k_{3z} k_s^4}$ and $L = \left(k_s^2 - 2k_{1x}^2\right) + 4k_{1x}^2 k_{pz} k_{sz}$

Where k_i is the complex propagation constant defined as:

$k_i = \omega/c_i + j\omega\alpha_i$ $\quad i=1,2,p,s$ and ω is the circular frequency.

k_{ix} and k_{iz} are respectively the projection of k_i on X-axis and Z-axis.

And R_{12}, R_{23} are the Fresnel reflection coefficients.

The Fresnel coefficients are independent of ω, the only dependence of $R(\omega,\theta)$ on the frequency comes from the phase factor introduced by the round-trip in the sediment. Therefore the frequency dependence will be defined with a proportionality factor uncertainty on the sediment thickness d.

HYDROPHONE RESPONSE MODELLING

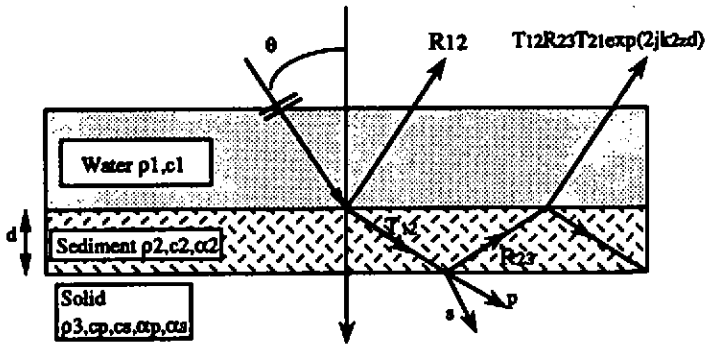

Figure 2.2: Geometrical approach of multiple reflections for the three layer bottom model.

As shown figure 2.3, for the two seabed configurations, for d=10 m and different frequencies, dependence on ω appears only for incidence angles below the critical angle. Oscillations are decreasing with frequency, hence for 10 kHz and d=10 m the curve is relatively smooth.

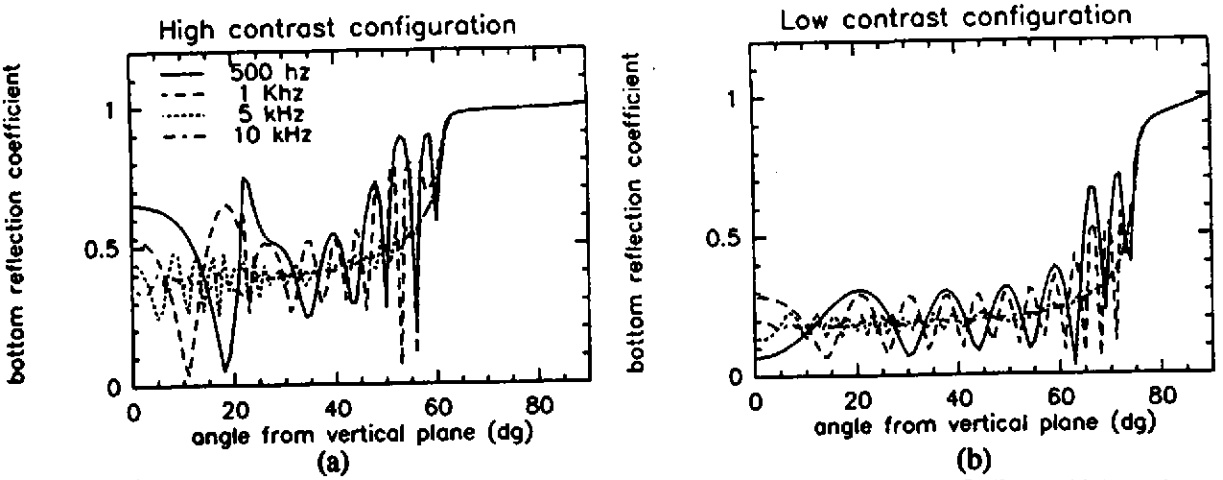

Figure 2.3: variations of bottom reflectivity coefficient with incident angle and frequency. Sediment thickness is set to 10 m. (a) for the high contrast configuration (HC), (b) for the low contrast configuration (LC) of bottom characteristics listed in table 2.1.

2.2 Estimation of the listening radius and the weighting function

We have defined the listening radius as the radius of the disk centered at the surface point above the hydrophone emitting 95% of the acoustic intensity received at the hydrophone location. This limited intensity is compared to the total intensity previously described as an infinite sum of image sources. As shown figure 2.4(a), each direction of propagation has a different number of image plane concerned. The boundaries are increasing when incidence angles tend to be vertical. In order to limit the CPU time, we have restricted number of image planes under the critical angle. This can be justified because as shown figure 2.3, in this case, R^n will rapidly tends to zero.

For the weighting function, we have to define the relative intensity arriving from different ranges at the sea surface. One source at a given range will radiate over $\pi/2$ radians in the vertical plane to the hydrophone and more the incidence is near the vertical incidence, more the order of the image plane will be high (figure 2.4(b)). We have applied a similar criterion to restrict the number of image

planes as previously for the listening radius. We have also considered a ponderation of each source area at a image plane relative to the surface source.

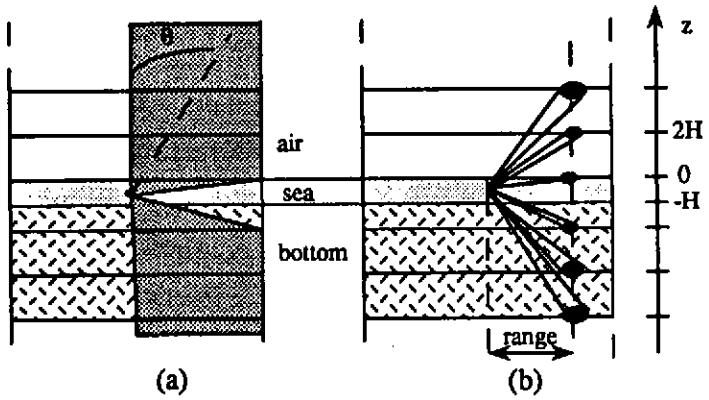

Figure 2.4(a): Configuration of sources points considered for a given listening radius. Number of image planes concerned varies from infinity to zero for respectively vertical and limit incident angle. This limit angle is determined by the straight line between the hydrophone and the surface source on the radius.
Figure 2.4(b): Location of sources to establish the weight at given distance. Ponderation has to be used to account for intensity per unit solid angle increasing surface area with the order of image.

3. HYDROPHONE MEASUREMENTS AND SURFACE AREA CONCERNED

We analyze now the dependence of the weighting function and listening radius on bottom characteristics, frequency and ocean depth. To better interpret bottom reflectivity influence on ambient noise, we have also considered the percentage of intensity arriving to the hydrophone without bottom reflection relative to the total intensity as defined previously as integer series.
Then we will insist on listening radius evolution with depth because this is the relevant parameter either for preparing an experiment or for interpreting data.

3.1 Dependence on bottom characteristics

The two seabed configurations have rather different behaviours, due to their reflectivity functions: The first difference is related to the variations of these functions with frequency, creating more or less oscillations below the critical angle (figure 2.3). Although this frequency dependence is determined with a factor uncertainty on the sediment thickness d, tests have shown that this parameter is not significant because oscillations are integrated for omnidirectional intensity. For d varying between 10 and 300 meters few variations are noticed for all parameters describing the surface area concerned by measurements.
In fact, the relevant parameter to explain bottom behaviours with frequency is the critical angle defined as: $\theta_c=\text{Arcsin}(c_1/c_2)$. Indeed above this angle, reflection is quasi total and mutipaths are propagating in these directions with a very high order of image plane. This is expressed by an important difference between frequencies for the high contrast configuration (figure 3.1): percentage of intensity varies from 6% to 94% between 500 Hz and 20 kHz while it is contained in the range 40% to 95% for the low contrast configuration (ocean depth=500m). This means also that the listening radius varies more rapidly with frequency for the high contrast configuration.

HYDROPHONE RESPONSE MODELLING

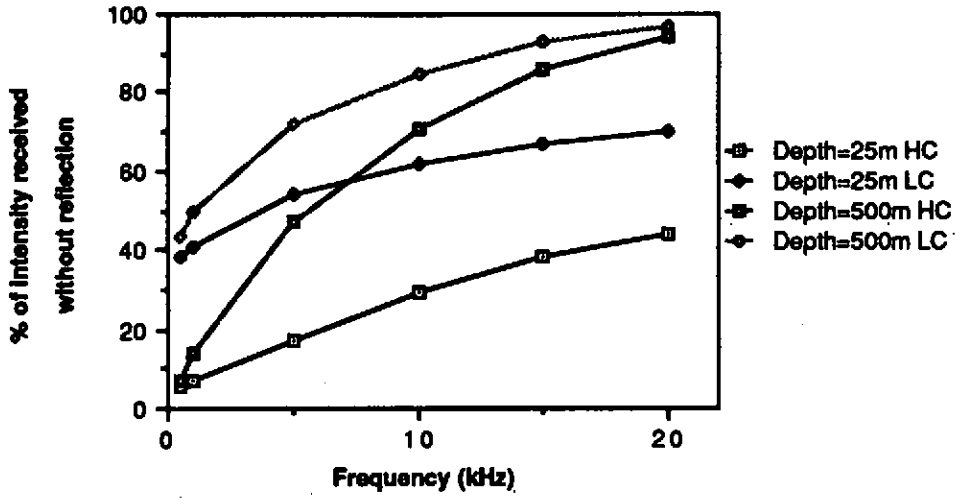

Figure 3.1: Percentage of intensity received without reflection for our extreme limits of ocean depth and the two bottom configurations. At low frequency, bottom characteristics are predominant as opposed to high frequency where seabed effect tend to vanish and ocean depth is dominant. LC and HC represent low and high contrast configurations.

3.2 Dependence on frequency and depth

As water absorption effects are dominant in regard to bottom reflectivity functions oscillations on omnidirectional noise dependence on frequency, multiple bounds decrease with depth and frequency. At low frequency, effects of reflection on the seabed are very significant: most of the sonic intensity arrives along multipath (up to several hundred of paths) and the weighting functions for low and high contrast configurations are very different from Farmer & Vagle's results without bottom reflection (see figure 3.2(a)), as opposed to higher frequencies (figure 3.2(b)).

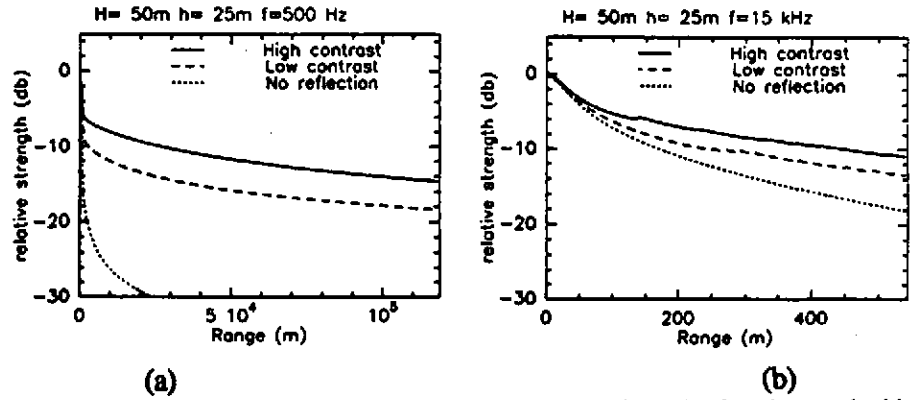

(a) (b)

Figure 3.2: Weighting functions compared for two different bottom reflectivity functions and without reflection as defined by Farmer and Vagle [1], (a) at low frequency 500 Hz and (b) at high frequency 15 kHz.

As this angle range increases (for example high contrast configuration compared to low one), at low frequency, more reflections have to be considered and the percentage of intensity arriving without

reflection (see figure 3.1) decreases, the listening radius (figure 3.3) increases. At high frequency, with water absorption, these multipaths are limited as much as frequency and depth increase.
Hence we can say that for very shallow water (depth < 50 m), bottom reflection is still acting at high frequency, while in deeper water conditions (depth > 300 m), it can be neglected for the higher frequency band.

3.3 Listening radius as a function of depth
We have chosen to study listening radius dependence on ocean depth rather than on hydrophone depth because for shallow water, it is very not very sensible when several paths occur. Depth of the ocean layer is varying between 25 m and 500 m, upper limit of a range where we do not consider refraction and hydrophone depth is set to half of the ocean depth.
On figure 3.3, listening radii as function of ocean depth are plotted for different frequencies and bottom configurations. We can derive from this figure an effect of seabed reflection on the listening radius which can either increase or decrease with depth. This phenomenom is due to opposed factors:
The first one will tend to increase the listening radius with depth: for a given propagation direction and number of reflections, when ocean depth is increasing, distance between image planes, and consequently surface sources, are moving off; the listening radius is also increasing. This is concerning low frequencies (< 5 kHz) , when water attenuation is not significant enough to reduce the number of sources representing the listening radius with depth.

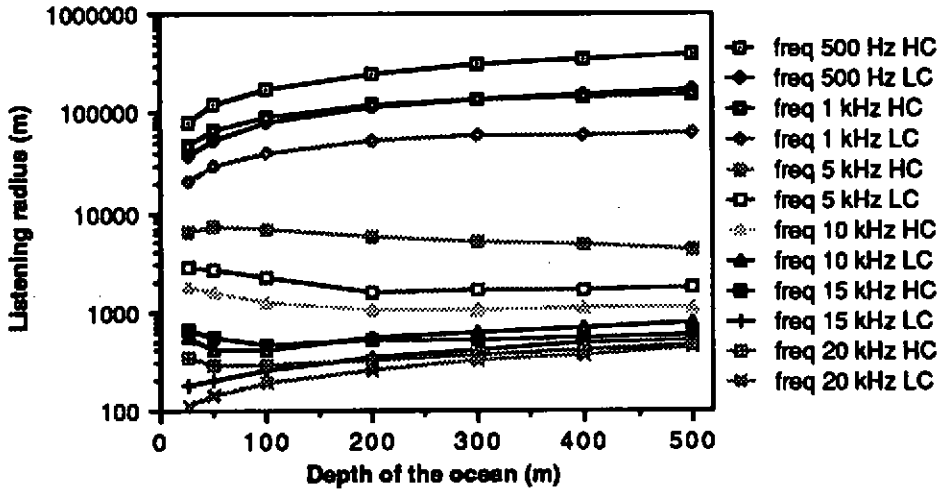

Figure 3.3: Listening radii as function of ocean depth in the frequency rang from 500 Hz to 20 kHz for the two kinds of bottom characreristics.

The second effect will be principal for higher frequencies: water attenuation will more deeply decrease the number of reflections necessary to contain 95% of intensity than the last surface sources will move off. Hence for frequencies between 5 kHz and 15 kHz, the listening radius is decreasing with depth, at least on the lower part of the depth range.
At last for very high frequencies, as we have observed previously, bottom reflectivity is insignificant and at 20 kHz or at 15 kHz for the higher depth, the listening radius has the same behaviour as Farmer & Vagle [1] have described.

3.4 Results discussion

With this simple model, taking into account seabed reflectivity, estimates of the listening radius seem to be qualitatively in agreement with observations, as well as they concern our last experiment and general observations of distant shipping at low frequency [6],[7].

Neverless variations of relative omnidirectional intensity, defined as the integral of directional noise or weighting function over the sea surface, as function of logarithmic frequency (see figure 3.4) point out the limits of our model to estimate hydrophone measurements. Indeed, previous observations of Knudsen [8] concerning ambient noise spectrum and its slope at -5 dB/oct and recent work of Medwin [9] about breaker spectra as sum of bubble spectra, joined together, imply that ocean plus bottom response should be quasi flat as function of frequency, independent of ocean depth, for sources radiating constant acoustic power P with frequency as we have supposed.

As shown figure 3.5, the slopes of omnidirectional noise vary with hydrophone depth and bottom characteristics which suggests disagreement with the generally observed Knudsen slope: Although variations due to bottom characteristics are not surprising at low frequency, such important variations of level and slope as function of depth have not been reported for higher frequency. This noise factor depending on the experimental site is also discussed in [10] without bottom reflection and it is proportional to $E_3(\alpha h)$ when refraction is neglected (E_3 is the exponential integral of third order). Hence significant variations of noise slope or level appear with hydrophone depth under these assumptions (see also on figure 3.4 plots without seabed reflection).

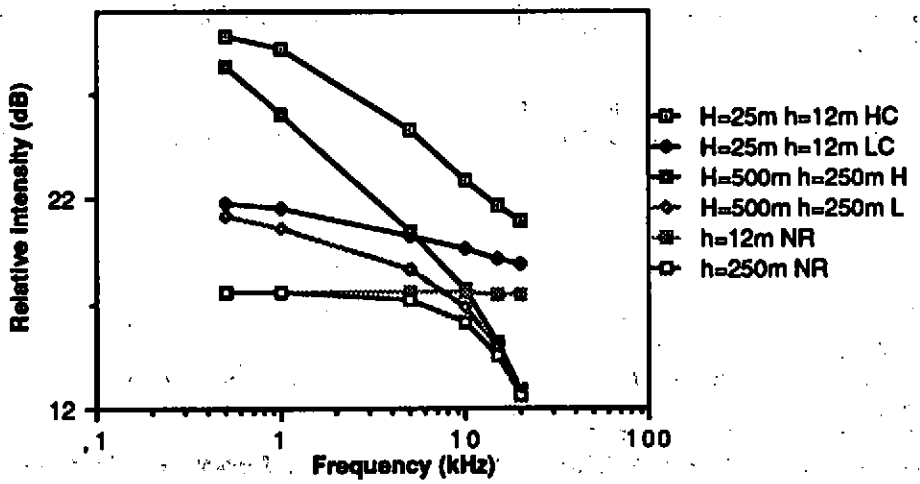

Figure 3.4: Comparaison of omnidirectional noise slopes as function of logarithmic frequency for the two seabed configurations LC, HC and without seabed reflection NR.

4 CONCLUSION

Hence, we have used a model of acoustic sources uniformly distributed at the sea surface to determine the weighting function and the listening radius above an hydrophone in shallow water. This geometrical model takes into account water absorption, reflection and attenuation at the bottom of the ocean. Two kinds of bottoms have been considered constituted of sediment and solid subbottoms, one corresponding to high contrast bottom and the second to low contrast bottom.

HYDROPHONE RESPONSE MODELLING

Results obtained will be usefull to interpret hydrophone use in coastal area. One mainly observes that:
- Percentage of intensity arriving to the hydrophone increases more or less rapidly as function of frequency and depth due to combined effects of water attenuation and bottom reflection. The main bottom characteristic being the critical angle. Due to multipaths seabed effects are significant; but more the water is shallow more the bottom reflection is important, the effect being negligeable for depth larger than 300 m in the higher part of the frequency range.
- The listening radius has been found not to be always increasing with depth but rather to increase or decrease due to opposed effects related to water absorption or bottom reflection explained by path variations due to bottom reflection.
- However, this model has been found to be too simple to synthesize an intensity spectrum close to Knusen "universal" spectrum.

More, these results do not take into account refraction in the water layer and the slope of the continental plateau which should tend to reduce differences between bottom configurations. Neither does it consider scattering as function of frequency on the rough bottom and surface which would have tendency to modify high frequency intensity.
For the future, we think of several ways of investigations:
First the use of the model to interpret undertaken experiment and to modify it if necessary as function of observations, trying to improve the physics.
Then the use of the model to analyse hydrophone network to consider problems as correlation between hydrophones at different spatial scales.
This study also indicates the interest to use directional hydrophone trying to limit bottom reverberation effects.

ACKNOWLEGMENTS: We would like to thank very much F Baudin, G Laurent and D Borie for their technical help during hydrophone experiments. This study has received support from CNET, DRET, INSU.

REFERENCES

[1] D M FARMER & S VAGLE, 'On the Determination of Breaking Surface Wave Distributions Using Ambient Sound', J Geophys res, 93 p3591-3600 (1988)
[2] D M F CHAPMAN, 'Surface-Generated Noise in Shallow Water: a Model', Proc I O A, 9 part 4 (1987)
[3] R BOHBOT, D LESSELIER and W TABBARA, 'Exact and Approximate Probing of Sea-Bottom', IEEE Ultrasonic Symposium, p333-338 (1989)
[4] H COX, 'Spatial Correlation in Arbitrary Noise Fields with Application to Ambient Sea Noise', JASA, 54 p1289-1301 (1973)
[5] L M BREKHOVSKIKH, 'Waves in Layered Media', 2nd Edition, T Robert trans, Academic Press, London p43 (1980)
[6] A J PERRONE, 'Deep-Ocean Ambient-Noise Spectra in the Northwest Atlantic', J Acoust Soc Am 46 p762-770 (1969)
[7] M. WENZ, 'Review of Underwater Acoustics Research: Noise', J Acoust Soc Am 51 p1010-1024 (1972)
[8] V O KNUDSEN, RS ALFORD and J W EMLING, 'Underwater Ambient Noise', J Marine Res, 7 p410-429 (1948)
[9] H MEDWIN & M M BEAKY, 'Bubble Sources of the Knudsen Sea Noise Spectra', J Acoust Soc Am, 86 p1124-1130 (1989)
[10] S VAGLE, W G LARGE and D M FARMER, 'An Evaluation of the WOTAN Technique of Interferring Oceanic Winds from Underwater Ambient Sound', J Atmos Oceanic Technol, 7 p576-595 (1990)